Journal of Molecular Structure 1197 (2019) 681–690

Contents lists available at ScienceDirect

Journal of Molecular Structure

journal homepage: http://www.elsevier.com/locate/molstruc

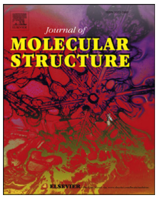

Molecular and crystal structures of tris(3-methylphenyl)phosphine and its chalcogenides

I.V. Sterkhova*, V.I. Smirnov, S.F. Malysheva, V.A. Kuimov, N.A. Belogorlova

A. E. Favorskii Irkutsk Institute of Chemistry, Siberian Division of Russian Academy of Sciences, 1 Favorskii Street 664033, Irkutsk, Russia

ARTICLE INFO

Article history:
Received 12 April 2019
Received in revised form
25 June 2019
Accepted 24 July 2019
Available online 26 July 2019

Keywords:
tris(3-methylphenyl)phosphine
tris(3-methylphenyl)phosphine
chalcogenides
Crystal structure
DFT calculations

ABSTRACT

The molecular and crystal structures of tris(3-methylphenyl)phosphine, tris(3-methylphenyl)phosphine oxide, tris(3-methylphenyl)phosphine sulfide and tris(3-methylphenyl)phosphine selenide were determined by X-ray diffraction. It was previously indicated that phosphine oxide should be isostructural with phosphine sulfide and phosphine selenide. However, this statement was not confirmed experimentally: the geometrical structure of the phosphine oxide is closer to the geometry of the phosphine. Tris(3-methylphenyl)phosphine, tris(3-methylphenyl)phosphine sulfide and tris(3-methylphenyl)phosphine selenide crystallize in the orthorhombic space group Pbca, while the phosphine oxide molecules in the crystal are packaged in the space group $Pca2_1$ with screw axis.

1. Introduction

Phosphines and their derivatives represent an important class of compounds for life sciences and the chemical industry [1]. In general, trivalent phosphines are used in numerous classic organic transformations [2–6], such as the Mitsunobu reaction [7], the Wittig reaction [8,9], Mukaiyama-Corey lactonization [10], the Appel reaction [11], Staudinger reaction [12] and so on. Furthermore, in organometallic chemistry they represent prime ligands to control most transition metal catalyzed reactions due to their excellent metal ligation properties. Functionalized triarylphosphines are widely used as ligands for transition metal complexes and as synthetic intermediates for the production of new materials [13].

For example, tolyl-substituted phosphine ligands are part of various transition metal complexes that catalyze various processes in industrial synthesis [14–19], are included in the meso-porous zeolite structures [20], and are used as new polymeric materials [21]. Copper (I) complexes with m-tolylphosphine ligands are promising for the production of OLEDs [22,23], Eu (III) clusters exhibit luminescent properties [24], and palladium complexes of tritolyl-substituted phosphines possess anti-bacterial and anti-cancer activity [25,26].

Tritolylphosphine chalcogenides have been used as ligands for transition metal catalysts that catalyze the epoxidation reaction [27], hydroformylation [28], for luminescent materials [24], as well as nonlinear optics [29], as building blocks, including restoration [30], C-H amidation [31] and ortho-alkenylation [32]. The Au (I) complexes of tritolylphosphine sulfide and selenide possess activity against rheumatoid arthritis [33].

Thus, the determination of the molecular structure of substituted phosphines and their chalcogenides and the study of the influence of the nature of substituents on the phosphorus atom both on the geometry of molecules and on the features of intermolecular binding in a crystal is an important task. Such studies are necessary to explain the physicochemical properties of the compounds under study, including their complexing ability, to evaluate and predict their reactivity. In this paper we discussed the features of the preparation, molecular and crystal structures of tris(3-methylphenyl)phosphine **1** and its chalcogenides: tris(3-methylphenyl)phosphine oxide **2**, tris(3-methylphenyl)phosphine sulfide **3** and tris(3-methylphenyl)phosphine selenide **4**.

---

* Corresponding author.
E-mail address: irina_sterkhova@irioch.irk.ru (I.V. Sterkhova).

https://doi.org/10.1016/j.molstruc.2019.07.094
0022-2860/© 2019 Published by Elsevier B.V.

2. Experimental section

2.1. Synthesis

2.1.1. Tris(3-methylphenyl)phosphine **1**

Tris (3-methylphenyl) phosphine 1 was synthesized according to the procedure given in the literature [34].

Colorless crystals, m.p. 134 °C (i-PrOH). FTIR (KBr, cm^{-1}): 3066, 3011, 2970, 2919, 2864, 1915, 1813, 1654, 1595, 1491, 1446, 1392, 1303, 1182, 1088, 1018, 807, 707, 620, 508. ^{1}H NMR (400.13 MHz, $CDCl_3$, δ, ppm): 2.36 (Me, 9H, s), 7.16 (3,5-H, C_6H_4, 6H, d, $^3J_{HH} = 7.5$ Hz), 7.23 (2,6-H, C_6H_4, 6H, t, $^3J_{HH} = 7.5$ Hz, $^3J_{PH} = 7.5$ Hz). ^{13}C NMR (100.62 MHz, $CDCl_3$, δ, ppm): 21.22 (Me), 129.21 (3,5-C, C_6H_4, d, $^3J_{PC} = 6.9$ Hz), 133.60 (2,6-C, C_6H_4, d, $^2J_{PC} = 19.5$ Hz), 134.16 (1-C, C_6H_4, d, $^1J_{PC} = 9.2$ Hz), 138.46 (4-C, C_6H_4). ^{31}P NMR (161.98 MHz, $CDCl_3$, δ, ppm): −7.63. For $C_{21}H_{21}P$ calcd (%): C, 82.87; H, 6.95; P, 10.18. Found: C, 82.84; H, 6.96; P, 9.98.

2.1.2. Tri(3-methylphenyl)phosphine oxide **2**

Phosphine **1** (0.22 g, 0.723 mmol) dissolved in EtOH (5 ml) and aq.H_2O_2 (34%, 0.075 g) was added and resulted mixture was stirred during 1 h at room temperature. In 1 h MnO_2 was added to quench the traces of H_2O_2. Then the mixture was filtered through K_2CO_3 and EtOH was removed in vacuum to give the phosphine oxide **2** as white powder.

Yield 0.229 g (99%). M.p. 148-150 °C (heptane), FTIR (KBr, cm^{-1}): 3024, 2921, 2862, 2819, 1922, 1820, 1656, 1599, 1499, 1444, 1399, 1310, 1175, 1115, 1025, 807, 660, 523, 464; ^{1}H NMR (400.13 MHz, $CDCl_3$, δ, ppm): 2.35 (Me, 9H, s), 7.16 (3,5-H, C_6H_4, 6H, br.d, $^3J_{HH} = 7.9$ Hz), 7.52 (2,6-H, C_6H_4, 6H, dd, $^3J_{HH} = 7.9$ Hz, $^3J_{PH} = 11.8$ Hz). ^{13}C NMR (100.62 MHz, $CDCl_3$, δ, ppm): 21.55 (Me), 129.14 (3,5-C, C_6H_4, d, $^3J_{PC} = 12.6$ Hz), 129.45 (1-C, C_6H_4, d, $^1J_{PC} = 107.5$ Hz), 132.10 (2,6-C, C_6H_4, d, $^2J_{PC} = 10.4$ Hz), 142.21 (4-C, C_6H_4, d, $^4J_{PC} = 2.8$ Hz); ^{31}P NMR (161.98 MHz, $CDCl_3$, δ, ppm): 27.49. For $C_{21}H_{21}PO$ calcd (%): C, 78.73; H, 6.61; P, 9.67. Found: C, 78.65; H, 6.59; P, 9.47.

2.1.3. Phosphine sulfide **3** and phosphine selenide **4**

Phosphine **1** (0.21 g, 0.69 mmol) was dissolved in Et_2O (5 ml) and elemental sulfur or selenium (0.70 mmol) was added and resulted mixture stirred during 1 h at room temperature. Then the mixture was filtered off and Et_2O was removed to give the phosphine chalcogenide **3** and **4** as powders.

2.1.4. Tri(3-methylphenyl)phosphine sulfide **3**

Yield 0.229 g (99%). M.p. 189-190 °C (i-PrOH). FTIR (KBr, cm^{-1}): 3018, 2920, 2865, 1921, 1819, 1654, 1595, 1494, 1444, 1396, 1304, 1184, 1100, 1023, 808, 687, 645, 578, 510, 440. ^{1}H ЯМР (400.13 MHz, $CDCl_3$, δ, ppm): 2.40 (Me, 9H, s), 7.24 (3,5-H, C_6H_4, 6H, dd, $^3J_{HH} = 8.2$ Hz, $^4J_{PH} = 2.7$ Hz), 7.61 (2,6-H, C_6H_4, 6H, dd, $^3J_{HH} = 8.2$ Hz, $^3J_{PH} = 13.1$ Hz). ^{13}C NMR (100.62 MHz, $CDCl_3$, δ, ppm): 21.10 (Me, d, $^5J_{PC} = 1.4$ Hz), 128.81 (3,5-C, C_6H_4, d, $^3J_{PC} = 12.9$ Hz), 129.74 (1-C, C_6H_4, d, $^1J_{PC} = 87.5$ Hz), 131.87 (2,6-C, C_6H_4, d, $^2J_{PC} = 11.1$ Hz), 141.48 (4-C, C_6H_4, d, $^4J_{PC} = 3.1$ Hz). ^{31}P NMR (161.98 MHz, $CDCl_3$, δ, ppm): 42.53. For $C_{21}H_{21}PS$ calcd (%):C, 74.97; H, 6.29; P, 9.21; S, 9.53. Found: C, 74.86; H, 6.27; P, 9.18; S, 9.41.

2.1.5. Tri(3-methylphenyl)phosphine selenide **4**

Yield 0.262 g (99%). M.p. 199-200 °C (i-PrOH). RTIR (KBr, cm^{-1}): 3043, 3026, 2920, 2859, 1914, 1645, 1595, 1494, 1444, 1394, 1305, 1184, 1097, 1021, 805, 704, 644, 625, 505, 438. ^{1}H NMR (400.13 MHz, $CDCl_3$, δ, ppm): 2.40 (Me, 9H, s), 7.23 (3,5-H, C_6H_4, 6H, dd, $^3J_{HH} = 8.1$ Hz, $^4J_{PH} = 2.9$ Hz), 7.61 (2,6-H, C_6H_4, 6H, dd, $^3J_{HH} = 8.1$ Hz, $^3J_{PH} = 13.6$ Hz). ^{13}C NMR (100.62 MHz, $CDCl_3$, δ, ppm): 21.37 (Me, d, $^5J_{PC} = 1.7$ Hz), 128.85 (1-C, C_6H_4, d, $^1J_{PC} = 79.2$ Hz), 129.12 (3,5-C, C_6H_4, d, $^3J_{PC} = 12.9$ Hz), 132.53 (2,6-C, C_6H_4, d, $^2J_{PC} = 11.2$ Hz), 141.85 (4-C, C_6H_4, d, $^4J_{PC} = 3.2$ Hz). ^{31}P NMR (161.98 MHz, $CDCl_3$, δ, ppm): 34.59 (s + d satellites: $^1J_{PSe} = 720.0$ Hz). ^{77}Se NMR (76.31 MHz, $CDCl_3$, δ, ppm): −260.47 (d, $^1J_{PSe} = 720.0$ Hz). For $C_{21}H_{21}PSe$ calcd (%): C, 65.80; H, 5.52; P, 8.08; Se, 20.60. Found: C, 65.72; H, 5.51; P, 7.98; Se, 20.12.

2.2. X-ray study and refinement

Single crystals of compounds **1, 3** and **4** were obtained by recrystallization from isopropanol, compound **2** – from heptane. Crystal data were collected on a Bruker D8 Venture diffractometer with MoKa radiation (l = 0.71073) using the φ and ω scans. The structures were solved and refined by direct methods using the SHELX programs set [35]. Data were corrected for absorption effects using the multi-scan method (SADABS). Nonhydrogen atoms were refined anisotropically using SHELX [35] (Sheldrick, 2008). All hydrogen atoms were found via Fourier difference maps. CCDC 1921474 (**1**), 1577514 (**2**), 1577515 (**4**), 1577516 (**3**) contain the supplementary crystallographic data for this paper. These data can be obtained free of charge from the Cambridge Crystallographic Data Centre via www.ccdc.cam.ac.uk/data_request/cif.

2.3. NMR spectroscopy

^{1}H, ^{13}C, ^{31}P NMR spectra were recorded on a Bruker DPX 400 MHz (400.13, 100.61, 161.98 and 76.31 MHz, respectively) with cyclohexane as an internal standard.

2.4. IR spectroscopy

The FTIR spectra were taken on a FTIR Spectrometer Varian 3100. For neutral compounds the spectra were recorded in KBr pellets.

3. Results and discussion

3.1. Synthetic features

Oxidation of phosphines (III) remains the most direct way to obtain phosphine-chalcogenides. The procedures for oxidation with elemental sulfur and selenium described in the literature proceed in benzene (toluene or chloroform) by boiling the reagents for 4-48 h [36,37].

In order to improve the method of obtaining phosphine-chalcogenides, we chose tris(3-methylphenyl)phosphine **1** as a model substrate, which was synthesized using the procedure given in literature [34]. Oxidation of phosphine **1** with elemental sulfur or selenium was carried out in diethyl ether, phosphine oxide was prepared by reacting phosphine **1** with hydrogen peroxide in EtOH. All experiments were performed at room temperature. It was established that when mixing of phosphine and oxidizing agents, the reaction with elemental sulfur or selenium ends in 1 h, and the reaction in EtOH also ends in 1 h at 40 °C.

In all experiments, yields of the obtained phosphine chalcogenides are about 99%. A comparison of our optimized real-time oxidation reaction conditions with those already described

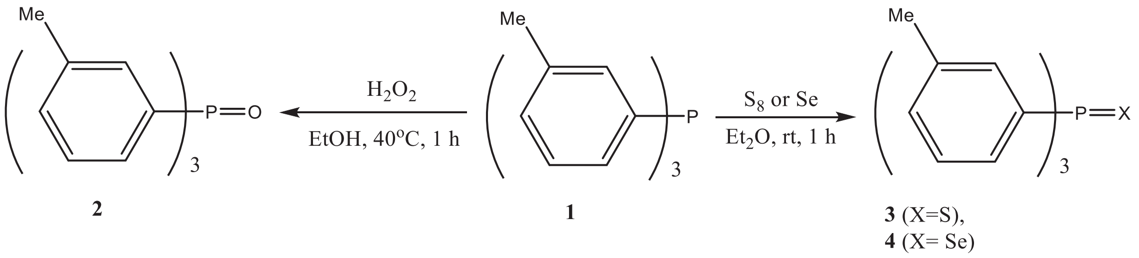

[36,37] shows that our system under the conditions of "mixing and stirring", as described above, is the fastest method and allows to obtain selectively pure tris(3-methylphenyl)phosphine chalcogenides. The proposed system does not contain additives and only a small stoichiometric excess of oxidant (sulfur, selenium or hydrogen peroxide) is used, the oxidation is completed faster than boiling in benzene or toluene.

3.2. *Structural analysis*

The molecular structures of phosphine **1** and its chalcogenides **2-4** are depicted in Fig. 1. Crystal data, data collection and structure refinement details are summarized in Table 1. Principal bond distances, bond angles and torsion angles are presented in Table 2.

The literature contains data on the molecular structure of tris(2-methylphenyl)substituted phosphine and its chalcogenides [38], tris(3-methylphenyl)substituted phosphine, its sulfide and selenide [39], and tris(4-methylphenyl)substituted phosphine selenide in the solid state [40]. However, the structures of these phosphines are mainly considered from the point of view of their participation as ligands in complexes with metals.

In the asymmetric units of compounds **1-4** there are one molecule, the disordering of methyl group (C19) is observed for **1** (Fig. 1). For the molecular structures of tri(3-methylphenyl)phosphine **1** and its halcogenides **2-4**, the characteristic propeller conformation type (Fig. 2) [41,42], in which two of the three repellent substituents are deployed symmetrically about the Cg-P axis for phosphine **1** and the Cg-P-(O, S, Se) axis for phosphine chalcogenides **2-4**. The torsion angles Cg1P1C1C2, Cg1P1C7C12 and Cg1P1C13C18 in phosphine **1** are −131.80, 129.31 and −142.85°, in phosphine oxide **2** -154.61, −57.57 and −22.94°, in phosphine sulfide **3** 166.17, −57.60 and −24.97° and in phosphine selenide **4** 165.47, −59.53 and −25.06° (Fig. 2a–d). This arrangement corresponds to *cis*, *cis*, *trans*- orientation of tolyl fragments with respect to the P = X bond (X = LP, O, S, Se) in compounds **1**–**4**. In phosphine **1**, the distance from the P atom to the centroid of the base of the C1C7C13 (Cg1) pyramid (Fig. 2a) is 0.815 Å; in compounds **2-4**, these distances are 0.692 Å, 0.690 Å and 0.686 Å, respectively (Fig. 2b–d). Thus, the height of the pyramid depends on the presence and nature of the substituent X at the phosphorus atom and decreases in the series: X = LP > O > S > Se. (LP = lone pair).

Geometrically, the crystal structure of the phosphine oxide molecule **2** is closer to the molecular structure of phosphine **1**, which contradicts the previously published data, which talked about the isostructural character of all chalcogen-substituted tris(3-methylphenyl)phosphine [39]. In compounds **1** and **2**, the two methyl groups of the tolyl substituents are turned towards LP of the phosphorus atom in phosphine **1**, and towards the oxygen atom in phosphine oxide **2**, one methyl group is turned in the opposite direction (Fig. 2a and b). In contrast, in the phosphine sulfide **3** and phosphine selenide **4** molecules, the methyl groups are different: one is turned in the direction of the heteroatom, and two in the opposite direction (Fig. 2c and d). The geometric characteristics of the molecular and crystalline structure of compounds **1**, **3**, and **4** are close to those established earlier [39].

The C–C bond lengths in compounds **1-4** are close to the average, in the phenyl fragments they range from 1.375 to 1.405 Å, in C-Me they are 1.502–1.512 Å. The average values of the angles C–P–C are 101.7, 106.4, 106.6, and 106.6° in compounds **1-4**, respectively, which is 3–8° less than the ideal pyramidal angle (109.5°). The average values of the C–P–X angles (where X = O, S and Se) in compounds **2-4** are close to 112.52, 112.55, and 112.20°, respectively, which is slightly greater than the ideal pyramidal angle.

The average value of P-C interatomic distance in phosphine **1** is 1.834 Å, the C-P-C angles are 101.72°, which is close to the values of these parameters in triphenylphosphine [43] (1.831 Å and 102.8°), tris(pyrenyl)phosphine [44] (1.838 Å and 102.38°) and tris(1-naphtalenyl)phosphine [45] (1.837 Å and 102.43°). In phosphine oxide **2**, the mean value of the P–C bond lengths is 1.806 Å, the P=O bond length is 1.492 Å, which is slightly different from the values in tris(pyrenyl)phosphine oxide [41] (1.826 (P-C) and 1.481 Å (P-O)), but very close to the values of the bonds P-C and P = O in triphenylphosphine oxide [46] (1.802 and 1.487 Å). In phosphine sulfide **3** and phosphine selenide **4**, the mean values of P-C bond lengths are very close and equal to 1.814 and 1.816 Å, respectively. The bond length of P=S in compound **3** is 1.957 Å, which is close to the values of this bond in such compounds as triphenylphosphine sulfide (1.950 Å) [47] and bis(2-(dimethylaminomethyl)phenyl) phenylphosphine sulfide (1.955 Å) [48]. The P=Se bond length in compound **4** is 2.105 Å, which is close to the values of this bond in other similar structures, for example, in tris(3-trifluoromethylphenyl)phosphine selenide (2.093 Å) [49] and in tris(4-fluorophenyl)phosphine selenide (2.110 Å) [50].

Thus, it can be seen from the above data that the length of the P–C bond in structures **1-4** is affected by the presence (or lack) of an heteroatom at the phosphorus atom, and the higher the electronegativity of this heteroatom, the shorter the P–C distance. Therefore, the P–C bond length decreases in row **1** > **4** > **3** > **2**: LP > Se > S > O.

Compounds **1**, **3** and **4** crystallize in the orthorhombic space group Pbca, **3** and **4** are isomorphic, their crystal lattice parameters are close to those described in Ref. [39], whereas crystal of **1** has completely different unit cell parameters. The molecules of compound **2** in the crystal are packed in the space group $Pca2_1$. Fragments of the crystal structures of compounds **1-4** are shown in Fig. 3(a–d).

The crystal structure of phosphines **1-4** is formed due to weak non-covalent interactions (Fig. 4a–d). In the crystal of compound **1**, the length of the short contacts C⋯H between the carbon atoms of the benzene ring and the hydrogens of the methyl groups of adjacent molecules is 2.869 Å (Fig. 4a). The shortest intermolecular contacts are observed between the oxygen atoms of phosphine oxide **2** and the hydrogen atoms of the methyl groups of the

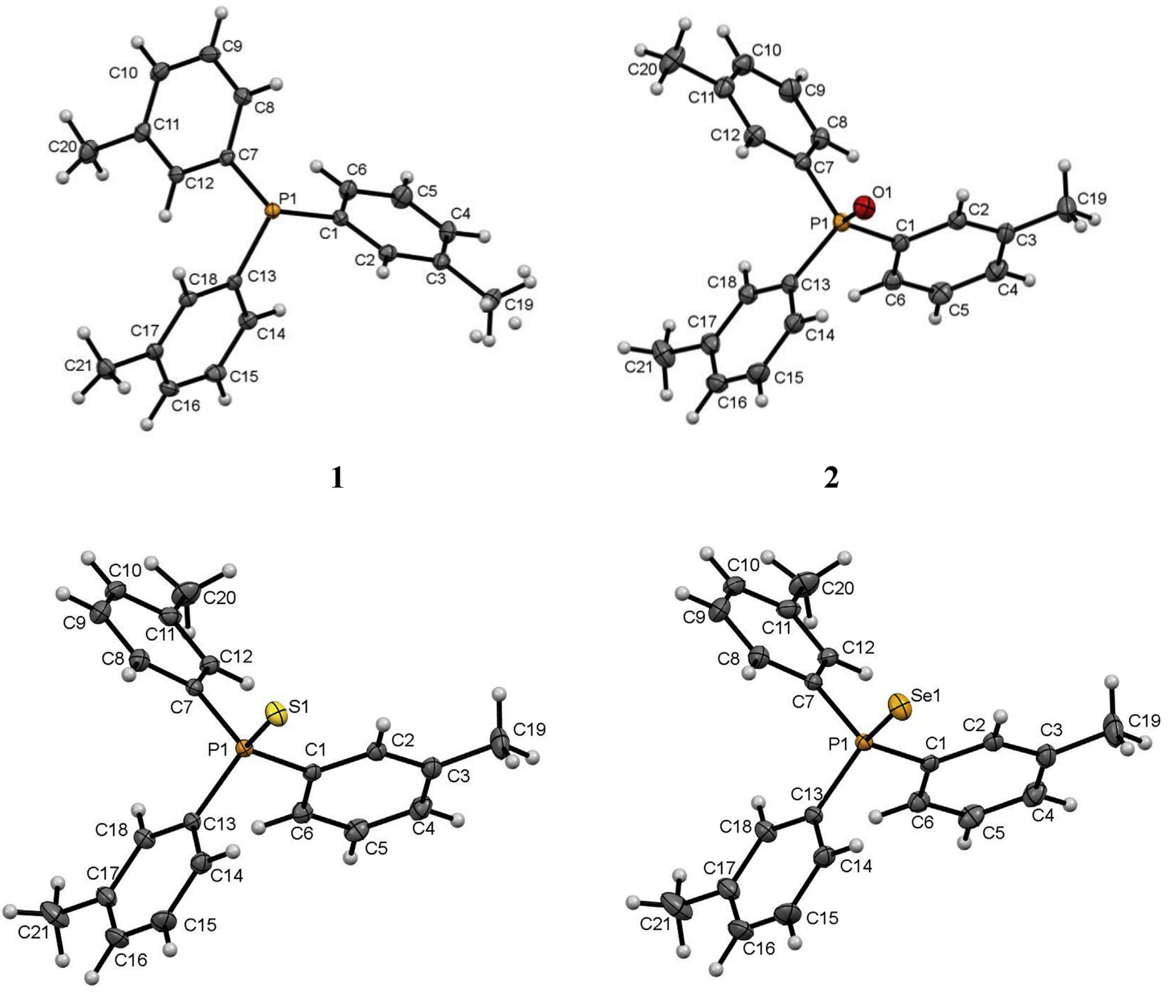

Fig. 1. Molecular structures of phosphine **1**, phosphine oxide **2,** phosphine sulphide **3** and phosphine selenide **4** (50% probability ellipsoids).

Table 1
Crystal data, details of measurements and structure refinement for compounds **1**–**4**.

Compound	1	2	3	4
Empirical formula	$C_{21}H_{21}P$	$C_{21}H_{21}PO$	$C_{21}H_{21}PS$	$C_{21}H_{21}PSe$
Mr, $g\cdot mol^{-1}$	304.35	320.35	336.41	383.31
Crystal system	orthorhombic	orthorhombic	orthorhombic	orthorhombic
Space group	P b c a	P c a 2_1	P b c a	P b c a
a/Å	15.945(2)	10.003(1)	10.234(1)	10.272(1)
b/Å	10.367(1)	15.144(2)	12.010(1)	12.276(1)
c/Å	20.031(1)	11.334(1)	29.064(2)	29.151(1)
α, β, γ, °	90, 90, 90	90, 90, 90	90, 90, 90	90, 90, 90
Volume/$Å^3$	3311.2(3)	1716.9(3)	3572.3(4)	3675.9(2)
Z	8	4	8	8
Density$_{calc}$/$g\cdot cm^{-3}$	1.221	1.239	1.251	1.385
Abs. coeff., mm^{-1}	0.161	0.162	0.268	2.127
2Θ range/°	4.80–60.14	4.88–60.09	4.86–60.16	5.35–60.14
Crystal size/mm	0.30 × 0.40 × 0.42	0.13 × 0.30 × 0.50	0.10 × 0.10 × 0.40	0.10 × 0.13 × 0.43
Crystal habit	colorless prism	colorless plate	colorless prism	colorless prism
F(000)	1296	680	1424	1568
Index ranges	$-22 \le h \le 22$, $-13 \le k \le 14$, $-28 \le l \le 21$	$-14 \le h \le 14$, $-21 \le k \le 21$, $-15 \le l \le 15$	$-14 \le h \le 14$, $-16 \le k \le 16$, $-40 \le l \le 40$	$-14 \le h \le 14$, $-17 \le k \le 17$, $-41 \le l \le 41$
Refl. collected	40607	80128	175774	132794
Indep. reflections	4858	5017	5250	5396
Max./min. transm.	0.7460/0.6690	0.8400/0.7600	0.7460/0.7076	0.7460/0.6222
Num. ref. param.	215	211	211	211
R_1/wR_2 [$I > 2\sigma(I)$]	0.0433/0.0959	0.0349/0.0773	0.0346/0.0818	0.0345/0.0727
R_1/wR_2 (all data)	0.0675/0.1057	0.0475/0.0827	0.0472/0.0885	0.0463/0.0766
Goodness-of-fit	1.033	1.065	1.051	1.125
Larg. diff. peak/hole, $e\cdot Å^{-3}$	0.408/−0.289	0.279/−0.200	0.342/−0.306	0.419/−0.384
Weight scheme, $P=(F_o^2+2F_c^2)/3$	$w = 1/[\sigma^2(F_o^2)+(0.0445\,P)^2+1.6469\,P]$	$w = 1/[\sigma^2(F_o^2)+(0.0352\,P)^2+0.4738\,P]$	$w = 1/[\sigma^2(F_o^2)+(0.0343\,P)^2+2.5537\,P]$	$w = 1/[\sigma^2(F_o^2)+(0.0259\,P)^2+3.4923\,P]$

Table 2
Selected bond lengths, bond and torsion angles in compounds **1**–**4**.

Bond	l, Å	Angle	φ, °	Torsion angle	θ, °
Compound **1**					
P1-C1	1.836(1)	C1-P1-C7	101.9(1)	C1-C2-C3-C4	1.3(2)
P1-C7	1.835(1)	C1-P1-C13	101.7(1)	C3-C2-C1-P1	−179.1(1)
P1-C13	1.832(1)	C7-P1-C13	101.7(1)	C13-P1-C7-C12	0.3(1)
C1-C2	1.405(2)	C1-C2-C3	121.7(1)	C1-P1-C7-C12	105.1(1)
C2-C3	1.397(2)	C2-C3-C4	118.3(1)	C3-C2-C1-C6	−0.6(2)
C3-C4	1.390(2)	C2-C1-P1	117.1(1)	P1-C1-C6-C5	178.0(1)
C4-C5	1.384(2)	C12-C7-P1	123.7(1)	C2-C3-C4-C5	−0.9(2)
Compound **2**					
O1-P1	1.492(2)	O1-P1-C1	111.9(1)	C1-C2-C3-C4	−0.4(3)
P1-C1	1.806(2)	O1-P1-C7	113.7(1)	C3-C2-C1-P1	−179.9(2)
P1-C7	1.804(2)	O1-P1-C13	112.0(1)	O1-P1-C1-C2	−26.1(2)
P1-C13	1.807(2)	C1-P1-C7	105.8(1)	O1-P1-C1-C6	154.0(2)
C1-C2	1.400(3)	C1-P1-C13	106.7(1)	C7-P1-C1-C6	−81.7(2)
C2-C3	1.393(3)	C7-P1-C13	106.3(1)	C13-P1-C1-C6	31.2(2)
C3-C4	1.393(3)	C1-C2-C3	121.7(1)	C2-C3-C4-C5	−0.6(3)
Compound **3**					
S1-P1	1.957(1)	S1-P1-C1	112.5(1)	C1-C2-C3-C4	−0.8(2)
P1-C1	1.817(1)	S1-P1-C7	112.0(1)	C3-C2-C1-P1	179.5(1)
P1-C7	1.811(1)	S1-P1-C13	112.5(1)	S1-P1-C1-C2	−14.3(1)
P1-C13	1.814(1)	C1-P1-C7	107.2(1)	S1-P1-C1-C6	164.6(1)
C1-C2	1.394(2)	C1-P1-C13	106.0(1)	C7-P1-C1-C6	−71.8(1)
C2-C3	1.395(2)	C7-P1-C13	106.1(1)	C13-P1-C1-C6	41.2(1)
C3-C4	1.392(2)	C1-C2-C3	121.4(1)	C2-C3-C4-C5	0.2(2)
Compound **4**					
Se1-P1	2.105(1)	Se1-P1-C1	112.6(1)	C1-C2-C3-C4	−1.0(3)
P1-C1	1.821(2)	Se1-P1-C7	111.7(1)	C3-C2-C1-P1	−179.7(1)
P1-C7	1.810(2)	Se1-P1-C13	112.3(1)	Se1-P1-C1-C2	−14.4(1)
P1-C13	1.816(2)	C1-P1-C7	106.8(1)	Se1-P1-C1-C6	165.2(1)
C1-C2	1.392(2)	C1-P1-C13	106.6(1)	C7-P1-C1-C6	−71.8(2)
C2-C3	1.392(3)	C7-P1-C13	106.5(1)	C13-P1-C1-C6	41.7(2)
C3-C4	1.394(3)	C1-C2-C3	121.4(2)	C2-C3-C4-C5	0.5(3)

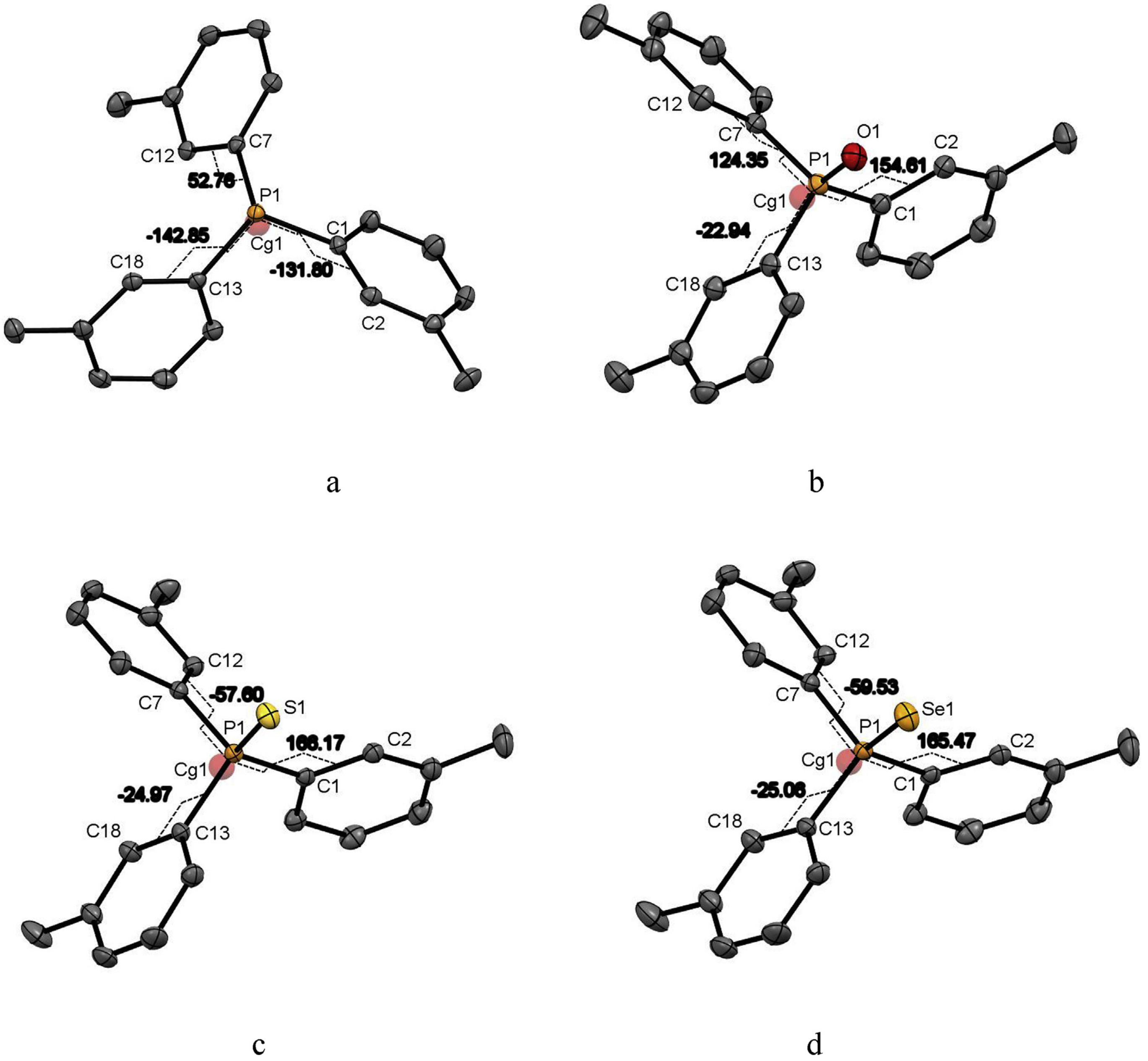

Fig. 2. Comparison of molecular geometry of **1**–**4** (a–d) (50% probability ellipsoids, H atoms are omitted for clarity).

neighboring molecules P═O···H–C, 2.5 Å in length (Fig. 4b).

In phosphine sulfide **3**, each molecule is associated with two adjacent molecules with short contacts formed by the sulfur atom with hydrogen atoms of the methyl and phenyl groups (2.814 and 2.910 Å) (Fig. 4c). Like phosphine sulfide, each molecule of phosphine selenide **4** is associated with two neighboring molecules by short contacts P═Se···HC (2.806 and 2.960 Å) (Fig. 4d).

3.3. DFT calculations

Theoretical studies of the spatial structure of phosphine and its chalcogenides with sterically bulky tolyl substituents at the phosphorus atom are also limited. For example, by the semi-empirical method PM3, the preferred conformers of tris(2-methylphenyl) phosphine and its chalcogenides were found [51], DFT calculated complexes of triphenylphosphine derivatives with zeolite Y [20] and evaluated the stability of tris(3-methylphenyl)phosphine complexes with Cu(I) [22]. The spatial structure of tris(3-methylphenyl)phosphine and its chalcogenides has been studied by the methods of dipole moments and quantum chemistry [52].

In order to study the effect of intramolecular electron interactions on bond lengths in compounds **1-4**, we performed quantum chemical calculations of their structures by the DFT method in the B3LYP/6-311 + G* basis using the Gaussian 09 suite of programs [53], NBO and MO analysis. The molecular orbital analysis is widely used to describe the electronic structure and chemical behavior of the different heteroatom compounds [54–56], including substituted phosphines [41]. Total optimization energies (-E), dipole moments, delocalization energy of electron density $E^{(2)}$, associated with charge transfer from lone pairs (LP) of phosphorus and chalcogen atoms to anti-binding σ*- orbitals, borderline energy values molecular orbitals HOMO, LUMO and the

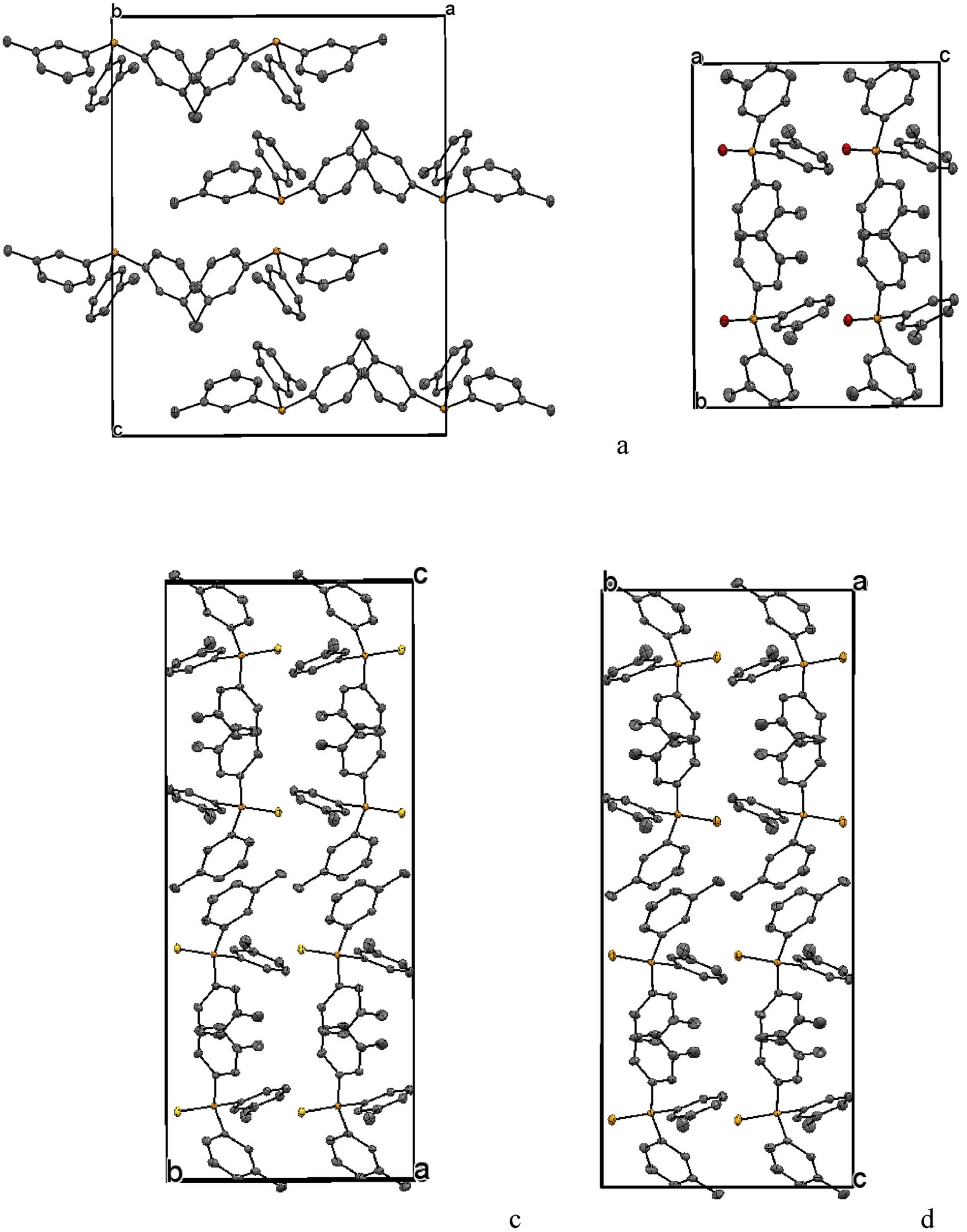

Fig. 3. Fragments of crystal packing of compounds **1-4**: a, d) view along *a0* axies; b, c) view along *0c* axies (ORTEP, H atoms are omitted for clarity).

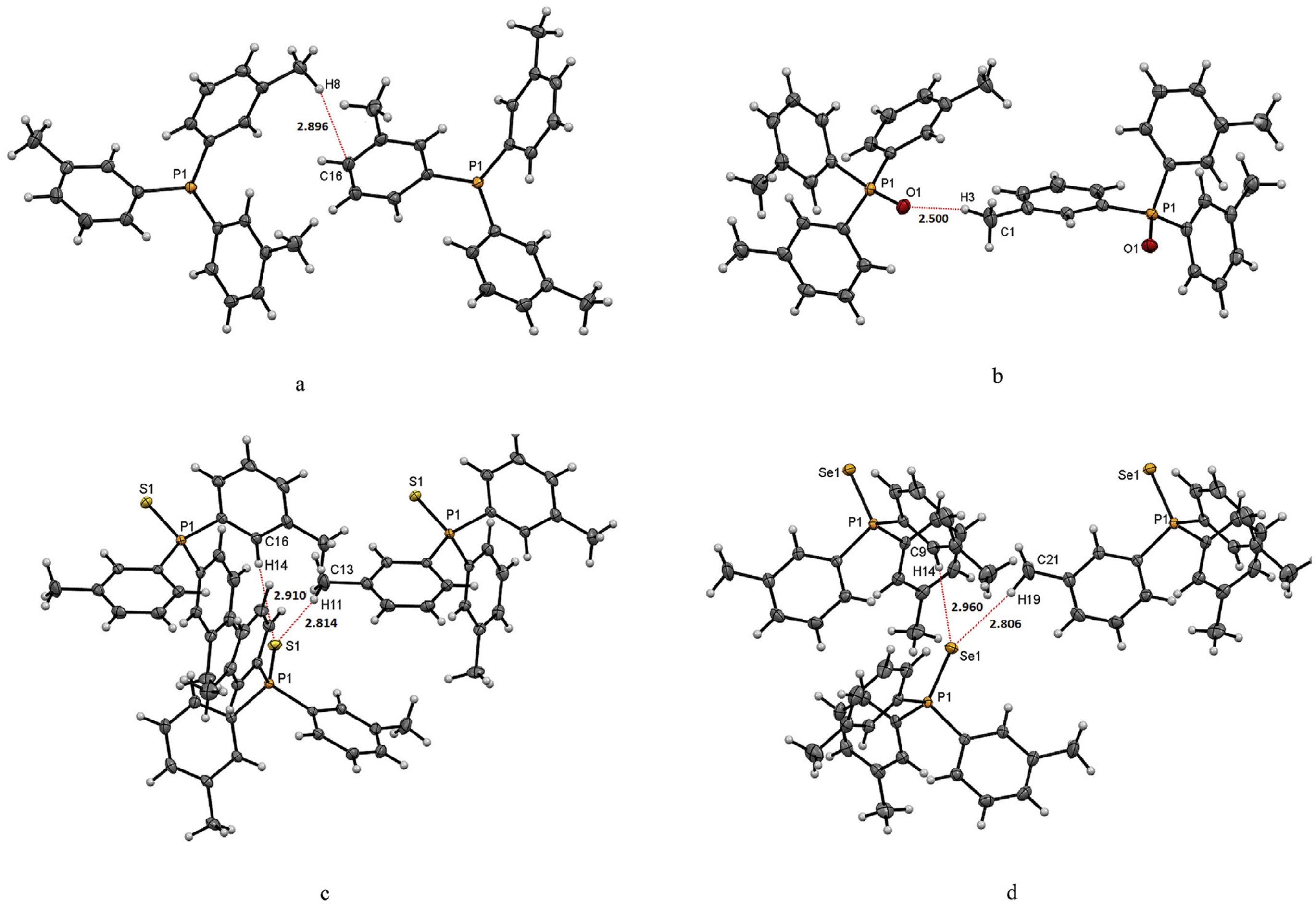

Fig. 4. Short contacts between molecules of compounds **1-4** in the crystal (ORTEP, 50% probability ellipsoids).

Table 3
MO and NBO analysis data for compounds **1**–**4**.

Characteristics	Compound			
	1	2	3	4
-E, a.u.	1154.4485534	1229.7249312	1552.6929795	3556.0281408
μ, D	1.50	4.13	5.44	5.60
$N_P \rightarrow \sigma^*_{C\text{-}C}$, $E^{(2)}$, kcal/mol	4.58 ÷ 4.87	0.53 ÷ 1.00	0.67 ÷ 0.86	0.69 ÷ 0.92
$N_X \rightarrow \sigma^*_{P\text{-}C}$, $E^{(2)}$, kcal/mol, X = O (**2**), S (**3**), Se (**4**)		12.24 ÷ 16.72	11.69 ÷ 14.42	10.51 ÷ 11.01
E_{LUMO}, eV	−0.84	−1.06	−1.14	−1.18
E_{HOMO}, eV	−5.88	−6.86	−5.90	−5.51
ΔE, eV	5.04	5.80	4.76	4.33

Table 4
Calculated (calc.) and experimental (exp.) bond lengths for compounds **1**–**4**.

Compound/Bond	1	2	3	4
P-X calc.	–	1.502(1)	1.979(1)	2.142(1)
P-X exp.	–	1.492(2)	1.957(4)	2.105(1)
P-C calc. (average)	1.854(1)	1.833(1)	1.842(1)	1.844(1)
P-C exp. (average)	1.837(2)	1.806(2)	1.814(1)	1.816(1)

corresponding energy gap ΔE, are given in Table 3.

According to the NBO analysis data, in compounds **2-4**, the maximum energy $E^{(2)}$ is observed for the intramolecular interaction of the LP of the oxygen atom with the σ*- orbitals of the P-C bond in compound **2**, while for the phosphine chalcogenides **3** and **4** the LP of sulfur and selenium atoms, respectively, is 2–4 kcal/mol lower.

In compound **1** the energy of interaction of the LP of the phosphorus atom with σ*- orbitals of C—C bonds is approximately 4.7 kcal/mol, in phosphine chalcogenides **2**-**4** the energies of this interaction decreases significantly and consist about 0.5–1.0 kcal/mol (Table 4). Thus, the calculated P—C bond lengths in compounds **1**–**4** increase in the series: **2** < **3** < **4** < **1**. Although the values of bond lengths for the gas phase are slightly overestimated (by 0.01–0.04 Å) compared to the experimental ones. From Table 4 it can be seen that calculated bond lengths are on 0.01–0.04 Å overrated in comparison with experimental.

As a rule, rather high values (>5 eV) of the energy difference between the main bound and unbound states of the molecule indicate a good chemical stability of the compounds under study.

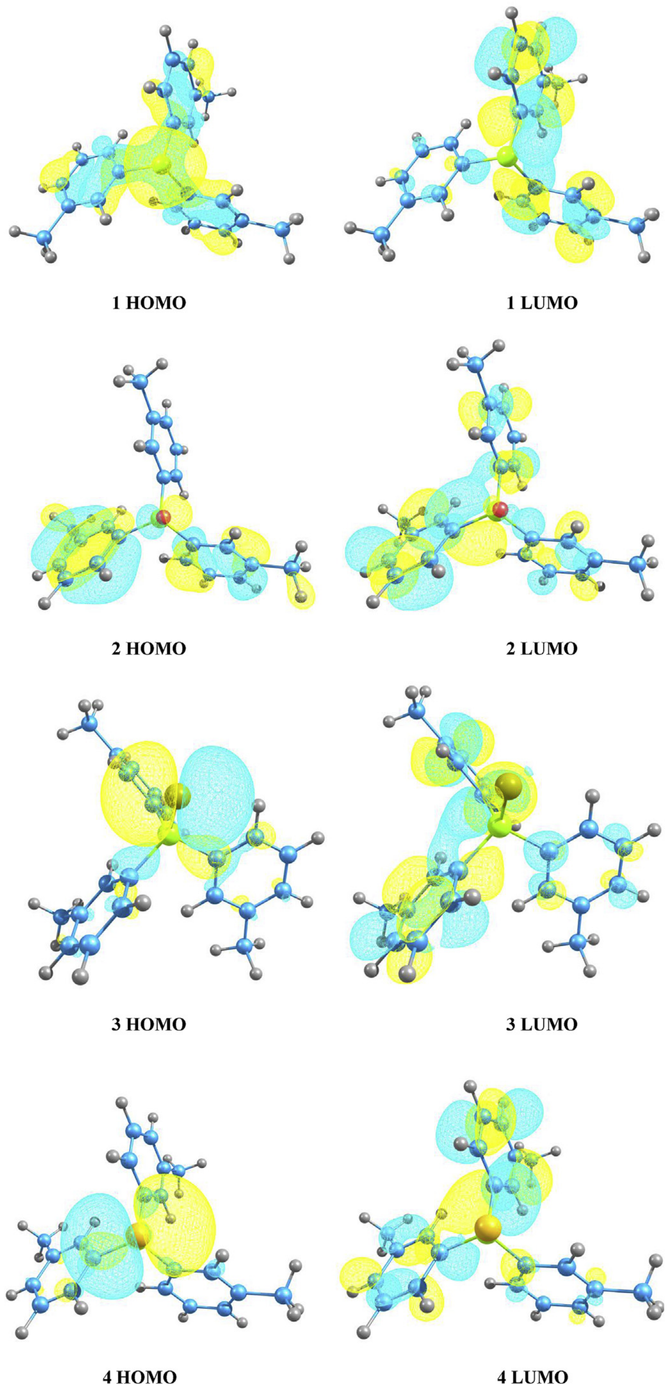

1 HOMO 1 LUMO

2 HOMO 2 LUMO

3 HOMO 3 LUMO

4 HOMO 4 LUMO

Fig. 5. Plots of frontier molecular orbitals for optimized structures of investigated compounds **1-4**.

Based on the data of Table 3, phosphine oxide **2** (ΔE = 5.8 eV) is the most stable among the studied compounds, and phosphine selenide **4** is the least stable (ΔE = 4.3 eV). The value of the dipole moment increases in the row **1** < **2** < **3** < **4**, which means an increase in the hydrophobic properties of these compounds.

Plots of frontier molecular orbitals for the studied molecules are shown in Fig. 5. As can be seen from Fig. 5, HOMO is characterized by delocalization of electron density on the LP of phosphorus (in phosphine **1**), oxygen, sulfur, and selenium (in phosphine chalcogenides **2-4**), and its smallest value corresponds to the LP of the oxygen atom in phosphine oxide **2**. In addition, in phosphine **1** it is evenly distributed on phenyl fragments. In contrast, in the phosphine chalcogenides **3** and **4**, electron density is mainly distributed on the LP of the S and Se atoms. Probably, the presence of such volumetric substituents as S and Se in compounds **3** and **4**, and the localization of the electron density of HOMO on them, determines their geometry, namely the rotation of the methyl group of the substituent in the opposite direction from the heteroatom. Unlike HOMO, LUMO are smaller and delocalized mainly on the phenyl rings of **1**–**4** molecules.

4. Conclusion

An optimized method for preparing tris(3-methylphenyl)phosphine chalcogenides was described. For the first time monocrystals of clear tris(3-methylphenyl)phosphine oxide (not co-crystals) were obtained and it's molecular structure was studied by X-ray analysis. The work shows the decisive influence of the nature of the substituent at the phosphorus atom in studied compounds on their molecular structure. The influence of O, S, and Se atoms on the change in the P – C bond length has been proved by X-ray diffraction and quantum chemical calculations. The calculated data indicate a decrease in the energy of intramolecular interaction of the phosphorus atom with tolyl substituents in phosphine chalcogenides compared with unsubstituted phosphine, which affects the lengths of P-C bonds in the structures under study. It is also shown that the crystal structures of **1**–**4** form by weak hydrogen bonds of the type CH···C, CH··O, CH···S and CH···Se.

Acknowledgement

The work was carried out using equipment of the Baikal Analytical Centre of SB RAS.

References

[1] L.D. Quin, A Guide to Organophosphorus Chemistry, John Wiely & Sons, Toronto, 2000.
[2] A. Börner (Ed.), Phosphorus Ligands in Asymmetric Catalysis: Synthesis and Application, Wiley-VCH, Weinheim, 2008.
[3] W.J. Tang, X.M. Zhang, Chem. Rev. 103 (2003) 3029–3069.
[4] K.V.L. Crepy, T. Imamoto, Top. Curr. Chem. 229 (2003) 1–40.
[5] L.W. Ye, J. Zhou, Y. Tang, Chem. Soc. Rev. 37 (2008) 1140–1152.
[6] C.J. O'Brien, J.L. Tellez, Z.S. Nixon, L.J. Kang, A.L. Carter, S.R. Kunkel, K.C. Przeworski, G.A. Chass, Angew. Chem. Int. Ed. 48 (2009) 6836–6839.
[7] D.L. Hughes, The Mitsunobu reaction, in: L.A. Paquette (Ed.), Org. React. vol. 42, 1992, pp. 335–656.
[8] P.A. Byrne, D.G. Gilheany, Chem. Soc. Rev. 42 (2013) 6670–6696.
[9] R.W. Hoffmann, Angew. Chem. Int. Ed. 40 (2001) 1411–1416.
[10] A. Parenty, X. Moreau, J.M. Campagne, Chem. Rev. 106 (2006) 911–939.
[11] R.M. Denton, J. An, B. Adeniran, A.J. Blake, W. Lewis, A.M. Poulton, J. Org. Chem. 76 (2011) 6749–6767.
[12] S. Shah, J.D. Protasiewicz, Coord. Chem. Rev. 210 (2000) 181–201.
[13] H.S. Lee, M. Takeuchi, M. Kakimoto, S.Y. Kim, Polym. Bull. 45 (2000) 319–326.
[14] H. Yoda, K. Nakatani, T. Terashima, M. Ouchi, M. Sawamoto, Macromolecules 43 (2010) 5595–5601.
[15] A. Dadrass, H. Rahchamani, J. Chil. Chem. Soc. 61 (2016) 2968–2972.
[16] G.J.S. Venter, A. Roodt, R. Meijboom, Inorg. Chim. Acta 362 (2009) 2475–2479.
[17] C. Xu, Y.X. Lu, X.H. Lou, Z.Q. Wang, W.J. Fu, B.M. Ji, Transit. Met. Chem. 36 (2011) 637–642.
[18] I. Fratoddi, M. Delfini, F. Sciubba, M.B. Hursthouse, H.R. Ogilvie, M.V. Russo, J. Organomet. Chem. 691 (2006) 5920–5926.
[19] T.S. Lobana, R. Kumar, R. Sharma, T. Nishioka, A. Castineiras, J. Coord. Chem. 58 (2005) 849–855.
[20] K. Okumura, M. Nakanishi, H. Takaba, Microporous Mesoporous Mater. 241 (2017) 400–408.
[21] K. Karami, S. Abedanzadeh, H. Farrokhpour, J. Lipkowski. J. Organomet. Chem. 805 (2016) 68–76.
[22] F. Bappler, M. Zimmer, F. Dietrich, M. Grupe, M. Wallesch, D. Volz, S. Brase, M. Gerhards, R. Diller, Phys. Chem. Chem. Phys. 19 (2017) 29438–29448.
[23] M. Wallesch, A. Verma, C. Flechon, H. Flugge, D.M. Zink, S.M. Seifermann, J.M. Navarro, T. Vitova, J. Gottlicher, R. Steininger, L. Weinhardt, M. Zimmer, M. Gerhards, C. Heske, S. Brase, T. Baumann, D. Volz, Chem. Eur J. 22 (2016) 16400–16405.

[24] K. Yanagisawa, Y. Kitagawa, T. Nakanishi, T. Akama, M. Kobayashi, T. Seki, K. Fushimi, H. Ito, T. Taketsugu, Y. Hasegawa, Eur. J. Inorg. Chem. 32 (2017) 3843–3848.

[25] S.Z. Khan, M.K. Amir, I. Ullah, A. Aamir, J.M. Pezzuto, T. Kondratyuk, F. Belanger-Gariepy, A. Ali, S. Khan, Zia-ur-Rehman, Appl. Organomet. Chem. 30 (2016) 392–398.

[26] I. Aziz, M. Sirajuddin, S. Nadeem, S.A. Tirmizi, Z. Khan, A. Munir, K. Ullah, B.A. Farooqi, H. Khan, M.N. Tahir, Russ. J. Gen. Chem. 87 (9) (2017) 2073–2082.

[27] R. Kino, K. Daikai, T. Kawanami, H. Furuno, J. Inanaga. Org. Biomol. Chem. 2 (2004) 1822–1824.

[28] J.-H. Choi, D.-H. Ko, S.-S. Eom, S.-G. Lee, M.-H. Hong, O.-H. Kwon, US8053605, 2011

[29] C.M. Whitaker, K.L. Kott, R.J. Mcmahon, J. Org. Chem. 60 (1995) 3499–3508.

[30] M. Kuroboshi, T. Kita, A. Aono, T. Katagiri, S. Kikuchi, S. Yamane, H. Kawakubo, H. Tanaka, Tetrahedron Lett. 56 (2015) 918–920.

[31] D. Gwon, D. Lee, J. Kim, S. Park, S. Chang, Chem. Eur J. 20 (2014) 12421–12425.

[32] M. Itoh, Y. Hashimoto, K. Hirano, T. Satoh, M. Miura, J. Org. Chem. 78 (2013) 8098–8104.

[33] S. Ahmad, A.A. Isab, H.P. Perzanowski, M.S. Hussain, M.N. Akhtar, Transit. Met. Chem. 27 (2002) 177–183.

[34] E. Le Gall, K. Ben Aissi, I. Lachaise, M. Troupel, Synlett 6 (2006) 954–956.

[35] G.M. Sheldrick, Acta Crystallogr. D 64 (2008) 112–122.

[36] S. Kawaguchi, Y. Minamida, T. Okuda, Y. Sato, T. Saeki, A. Yoshimura, A. Nomoto, A. Ogawa, Adv. Synth. Catal. 357 (2015) 2509–2519.

[37] A.P. Cinderella, B. Vulovic, D.A. Watson, J. Am. Chem. Soc. 139 (2017) 7741–7744.

[38] T.S. Cameron, B. Dahlen, J. Chem. Soc., Perkin Trans. 2 15 (1975) 1737–1751.

[39] T.S. Cameron, K.D. Howlett, K. Miller, Acta Crystallogr. B 34 (1978) 1639–1644.

[40] A. Muller, Acta Crystallogr. 67 (2011) o45.

[41] A.V. Artem'ev, E.P. Doronina, M.I. Rakhmanova, A.O. Sutyrina, I.Y. Bagryanskaya, P.M. Tolstoy, A.L. Gushchin, A.S. Mazur, N.K. Gusarova, B.A. Trofimov, New J. Chem. 40 (2016) 10028–10040.

[42] B.A. Trofimov, N.K. Gusarova, A.V. Artem'ev, S.F. Malysheva, N.A. Belogorlova, A.O. Korocheva, O.N. Kazheva, G.G. Alexandrov, O.A. Dyachenko, Mendeleev Commun. 22 (2012) 187–188.

[43] B.J. Dunne, A.G. Orpen, Acta Crystallogr. C47 (1991) 345–347.

[44] K. Behm, J.B. Essner, C.L. Barnes, G.A. Baker, J.R. Walensky, Dalton Trans. 46 (2017) 10867–10875.

[45] W.L. Davis, A. Muller, Acta Crystallogr. 68 (2012) o3484.

[46] P. Tinnemans, P. White, S. Rijpkema, CSD Communication (Private Communication), CCDC, 2017, 1562959.

[47] W. Dreissig, K. Plieth, P. Zaske, Acta Crystallogr. B 28 (1972) 3473–3477.

[48] A. Rotar, A. Covaci, A. Pop, A. Silvestru. Revue Roumaine De Chimie 55 (2010) 823–829.

[49] D.W. Allen, L.A. March, I.W. Nowell, J. Chem. Soc. Dalton Trans. 3 (1984) 483–485.

[50] N.A. Barnes, S.M. Godfrey, R.T.A. Halton, R.Z. Khan, S.L. Jackson, R.G. Pritchard, Polyhedron 26 (15) (2007) 4294–4302.

[51] I. Yavari, V. Hadigheh-Rezvan, Phosphorus&Sulfur&Silicon 174 (2001) 151–162.

[52] R.R. Ismagilova, A.A. Kuznetsova, D.V. Chachkov, S.F. Malysheva, N.A. Belogorlova, Y.A. Vereshchagina, Russ. J. Gen. Chem. 88 (11) (2018) 2251–2256.

[53] M.J. Frisch, G.W. Trucks, H.B. Schlegel, G.E. Scuseria, M.A. Robb, J.R. Cheeseman, G. Scalmani, V. Barone, B. Mennucci, G.A. Petersson, H. Nakatsuji, M. Caricato, X. Li, H.P. Hratchian, A.F. Izmaylov, J. Bloino, G. Zheng, J.L. Sonnenberg, M. Hada, M. Ehara, K. Toyota, R. Fukuda, J. Hasegawa, M. Ishida, T. Nakajima, Y. Honda, O. Kitao, H. Nakai, T. Vreven, J.A. Montgomery, J.E. Peralta, F. Ogliaro, M. Bearpark, J.J. Heyd, E. Brothers, K.N. Kudin, V.N. Staroverov, R. Kobayashi, J. Normand, K. Raghavachari, A. Rendell, J.C. Burant, S.S. Iyengar, J. Tomasi, M. Cossi, N. Rega, J.M. Millam, M. Klene, J.E. Knox, J.B. Cross, V. Bakken, C. Adamo, J. Jaramillo, R. Gomperts, R.E. Stratmann, O. Yazyev, A.J. Austin, R. Cammi, C. Pomelli, J.W. Ochterski, R.L. Martin, K. Morokuma, V.G. Zakrzewski, G.A. Voth, P. Salvador, J.J. Dannenberg, S. Dapprich, A.D. Daniels, O. Farkas, J.B. Foresman, J.V. Ortiz, J. Cioslowski, D.J. Fox, Gaussian 09, Revision B.01, Gaussian Inc, Wallingford, CT, 2009.

[54] M.F. Zaltariov, C. Cojocaru, S. Shova, L. Sacarescu, M. Cazacu, J. Mol. Struct. 1120 (2016) 302–316.

[55] P. Gautam, O. Prakash, R.K. Dani, M.K. Bharty, N.K. Singh, R.K. Singh, J. Mol. Struct. 1127 (2017) 489–497.

[56] I.V. Sterkhova, I.M. Lazarev, N.F. Lazareva, J. Mol. Struct. 1184 (2019) 200–206.